BIOTECHNOLOGY AND BIOENGINEERING
VOL. XII, PAGES 747–769 (1970)

A Dynamic Mathematical Model of the Chemostat*

**T. B. YOUNG, D. F. BRULEY, and H. R. BUNGAY, III,
Clemson University, Clemson, South Carolina 29631

Summary

A number of experimental studies on the dynamic behavior of the chemostat have shown that the specific growth rate does not instantaneously adjust to changes in the concentration of limiting substrate in the chemostat following disturbances in the steady state input limiting substrate concentration or in the steady state dilution rate. Instead of an instantaneous response, as would be predicted by the Monod equation, experimental studies have shown that the specific growth rate experiences a dynamic lag in responding to the changes in the concentration of limiting substrate in the culture vessel. The observed dynamic lag has been recognized by researchers in such terms as *an inertial phenomenon* and as *a hysteresis effect*, but as yet a systems engineering approach has not been applied to the observed data. The present paper criticizes the use of the Monod equation as a dynamic relationship and offers as an alternative a dynamic equation relating specific growth rate to the limiting substrate concentration in the chemostat. Following the development of equations, experimental methods of evaluating parameters are discussed. Dynamic responses of analog simulations (incorporating the newly derived equations) are compared with the dynamic responses predicted by the Monod equation and with the dynamic responses of experimental chemostats.

INTRODUCTION

The dynamic behavior of microorganisms is of both engineering and fundamental scientific interest. Bioengineers are primarily concerned with microbial dynamics from the standpoint of process control. An understanding of the unsteady state behavior of microbial processes is essential if engineers are to design effective control

* Supported by PHS Research Traineeship.

** Presented in part at the 157th National Meeting, American Chemical Society, New York, N. Y., September, 1969.

systems. On the other hand, bioscientists are interested in microbial dynamics because research in this area promises to render valuable information on the mechanisms involved in microbial growth and reproduction. In the present paper interest is restricted to the dynamic behavior of the chemostat continuous culture although the approach taken is equally applicable to other microbial processes.

Dynamic Behavior of the Chemostat

In attempting to predict the dynamic behavior of the chemostat most workers have used variations on the well-known Monod model. The basic Monod model consists of the equations

$$(dX/dt) = \mu X - DX \tag{1}$$

$$(dS/dt) = DS_o - DS - (\mu X/Y) \tag{2}$$

$$\mu = \hat{\mu}(S/K_s + S) \tag{3}$$

where: X = cell mass concentration, mass/volume

S = output limiting substrate concentration, mass/volume

S_o = input limiting substrate concentration, mass/volume

D = dilution rate, time^{-1}

μ = specific growth rate, time^{-1}

$\hat{\mu}$ = maximum specific growth rate, time^{-1}

Y = yield coefficient, mass cells/mass limiting substrate

K_s = saturation constant, mass/volume

Variations on the basic Monod model have accounted for varying yield coefficients by use of the equation

$$(1/Y_o) = (1/Y) + (K/\mu) \tag{4}$$

where: Y_o = observed yield coefficient

K = factor for maintenance energy

Other variations have algebraically modified equation (3) to account for substrate inhibition.[1] The dynamic behavior of the chemostat at predicted by equations (1), (2), and (3) and by equations (1), (2), (3), and (4) has been summarized by Koga and Humphrey.[2] The

Monod model has not been successful in predicting the dynamic behavior of experimental chemostats. Contrary to the instantaneous relationship implied by equation (3) the experimental studies of Mateles et al.,[3] Aiba et al.,[4,5,6] Storer and Gaudy,[7] Gilley and Bungay,[8,9] and Young and Bruley,[10] have all demonstrated that the specific growth rate of microbial cells growing in a chemostat does not instantaneously adjust to changes in the limiting substrate concentration, S, following disturbances in the steady state values of dilution rate, D, or in the steady state values of the input limiting substrate concentration, S_o. Yasuda and Mateles[11] were first to show that the specific growth rate does not instantaneously adjust to twofold positive step changes in dilution rate. In a chemostat consisting of *E. coli B* (wild type) growing on synthetic nitrogen-limited and glucose-limited media it was concluded that the specific growth rate of the cells could increase immediately by a small amount, but that further increases to the new higher steady state value took several hours.

Similarly, in a comprehensive study on a chemostatic culture of *Azobacter vinelandi*, Aiba et al.[4,5,6] has shown that specific growth rate responses lag the responses of S following both positive and negative step changes in D. One of the more significant observations reported in this work is that of an *inertial phenomenon* in which cell concentrations rose to values higher than those predicted by the Monod model. This inertial effect is in fact well explained by a lag in the specific growth rate response to a decreasing value of S. Storer and Gaudy[7] have reported data on the transient responses of a mixed culture chemostat growing on synthetic glucose minimal medium that again demonstrates the presence of a dynamic lag in the response of specific growth rate to changes in the glucose concentration in the chemostat. Following threefold increases in S_o a *hysteresis effect* was noted in the specific growth rate response. Growth rate hysteresis is a concept originally developed by Perret.[12] The hysteresis can be explained by a lag in specific growth rate adjustment to rapid increases or decreases in S. Dynamic studies on a glucose-limited chemostatic culture of *S. cerevisiae* have also confirmed the presence of a lag in specific growth rate response to glucose concentration changes resulting from square wave changes in S_o and from step changes in D.[8,9,10] In conclusion, a number of studies on different chemostats have indicated that while specific

growth rate can initially respond instantaneously by a relatively small amount to changes in S, further adjustments occur relatively slowly and tend to lag the changes in S.

Evaluation of the Dynamic Aspects of the Monod Equation

Having concluded that experimental dynamic data do not agree with the instantaneous algebraic relationship of equation (3), the question arises "Should the Monod equation be expected to predict dynamic behavior in a chemostat.?" This question can be answered by considering the origin of the Monod equation and giving a little thought to its true meaning. The development of the Monod equation and the experimental determination of $\hat{\mu}$ and K_s have been discussed by a number of workers, most notably Herbert *et al.*[13] Regardless of whether $\hat{\mu}$ and K_s are determined from batch culture or steady state continuous culture data, the Monod equation as it applied to a continuous culture defines a series of steady states or equilibrium conditions at which a given culture can operate. At each point on the Monod curve all of the mechanisms involved in growth and reproduction, such as mass transfer across the cytoplasmic membrane, formation of biochemical monomers, and the subsequent macromolecular synthesis, have established constant rates which are in turn manifested in a steady specific growth rate. In this sense the Monod equation, as applied to continuous cultures, is analogous to a thermodynamic equation of state that defines a space of equilibrium states. It logically follows then that the rate of transition between states in a chemostat can no more be accurately predicted by the Monod equation than a thermodynamic equation of state can predict the rate of attaining thermodynamic equilibrium. Another way of stating this idea is that transition between two steady states does not necessarily follow a pathway drawn through a series of equilibrium points. In fact, in the chemostat the only way such a transition could occur would be if all the mechanisms involved responded in a uniform transient manner to changes in S. This possibility seems unlikely if not impossible. More likely what does occur upon a disturbance in S is that each mechanism involved in cell growth and reproduction responds at its own rate and in a sequence determined by its relative kinetic position. In view of these considerations the Monod equation would not be expected to apply during transient conditions in a chemostat. In addition, models incorporating

algebraic modifications of the Monod equation for cases such as substrate inhibition would not be expected to be valid during unsteady state operation.[1] Even models that incorporate hysteresis loops in growth rate response are limited to describing transient behavior to a particular disturbance at a particular steady state.[7] It is evident from the above discussion that a dynamic relationship exists between μ and S during transients in a chemostat, that is

$$\mu = f(S,t) \tag{5}$$

This idea has been appreciated in only a few past studies.[14,15] Perhaps this results from the fact that most studies have failed to approach the problem of developing a dynamic mathematical model of the chemostat from a systems engineering point of view. This is the approach that will be taken in the present paper.

A DYNAMIC MODEL OF THE CHEMOSTAT

A Systems Engineering Approach

The systems engineering approach to developing a dynamic mathematical model of a physical process begins by the formulation of a block diagram. The block diagram is a convenient way of expressing how system variables are related or "how the system works." A linear block diagram for the chemostat in Figure 1 can be developed as follows:

Mass balances on limiting substrate and cell masses entering and leaving the chemostat give the equations

$$V(dS/dt) = FS_o - FS - (\mu XV/Y) \tag{6}$$

$$V(dX/dt) = \mu XV - FX \tag{7}$$

where: V = volume of chemostat

F = volumetric flow rate.

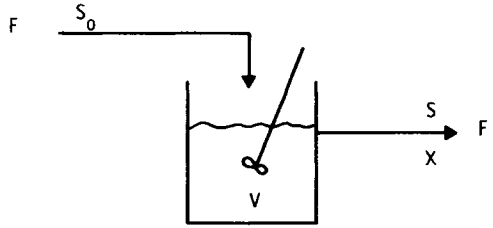

Fig. 1. Schematic diagram of chemostat.

The assumption is made that the specific growth rate is dynamically related to limiting substrate as expressed by the general equation

$$\mu = f(S,t). \tag{5}$$

Equations (6) and (7) can be rearranged to the forms

$$\theta(dS/dt) + S = S_o - (\mu\theta X/Y) \tag{8}$$

$$(dX/dt) = [\mu - (1/\theta)]X \tag{9}$$

where: $\theta = (1/D)$.

The deviation variables $\bar{S},\bar{X}$, and $\bar{\mu}$ are defined by the equations

$$\bar{X} = X - X_s \tag{10}$$

$$\bar{S} = S - S_s \tag{11}$$

$$\bar{\mu} = \mu - \mu_s = \mu - (1/\theta) \tag{12}$$

where: s subscript denotes steady state values.
Substitution of equations (10), (11), and (12) into equations (8) and (9) gives the deviation equations

$$\theta(d\bar{S}/dt) + \bar{S} = \bar{S}_o - (\theta/Y)(\mu_s\bar{X} + \bar{\mu}X_s + \bar{\mu}\bar{X}) \tag{13}$$

$$(d\bar{X}/dt) = \bar{\mu}X_s + \bar{\mu}\bar{X}. \tag{14}$$

Neglecting the products of deviation variables gives

$$\theta(d\bar{S}/dt) + \bar{S} = \bar{S}_o - (\theta/Y)(\mu_s\bar{X} + \bar{\mu}X_s) \tag{15}$$

$$(d\bar{X}/dt) = \bar{\mu}X_s. \tag{16}$$

Taking the Laplace transform of equations (15) and (16) gives

$$\bar{S}(s) = \{\bar{S}_o(s) - (\theta/Y)[\mu_s\bar{X}(s) + \bar{\mu}(s)X_s]\}(1/\theta_s + 1) \tag{17}$$

$$\bar{X}(s) = \bar{\mu}(s)(X_s/s). \tag{18}$$

From equation (5) a general Laplace domain equation might be written

$$\bar{\mu}(s) = G(s)\bar{S}(s). \tag{19}$$

From equations (17), (18) and (19) it can be seen that the chemostat can be represented by a closed loop block diagram as shown in Figure 2. The block diagram is made up of five blocks or transfer functions:

G_1, G_2, G_3, G_4, and G_5. G_1 is a transfer function for a first order mixing process where θ is the residence time of the chemostat. G_2 represents the dynamic relationship between $\bar{S}$ and $\bar{\mu}$. G_3 relates the growth rate term to the output variable $\bar{X}$. G_4 and G_5 represent transfer functions for the negative feed back loops and are analogous to the transfer functions representing sensor dynamics in conventional control systems. The signal emerging from the algebraic addition junction, $\overline{\Delta S}$, is a substrate consumption term. The negative feedback loops are responsible for the observed self-adjusting or stability properties of the chemostat. The output signal emerging from the algebraic subtraction junction is analogous to an error term from a controller in a conventional closed looped control system.

Several limiting assumptions were made in arriving at the block diagram of Figure 2. First, equations (13) and (14) were linearized. Also θ and Y were assumed to be constants. Thus, when perturbations are large or when θ or Y vary in time, the linear block diagram would not apply. In spite of these limitations the block diagram is valuable in that it enables one to visualize the relationships between system variables and it reveals the closed loop nature of the chemostat.

Determination of the Dynamic Relationship Between $\bar{\mu}$ and $\bar{S}$

From the previous discussion it should now be evident that the core of the problem of developing an accurate dynamic model of the chemostat lies in the determination of the dynamic relationship

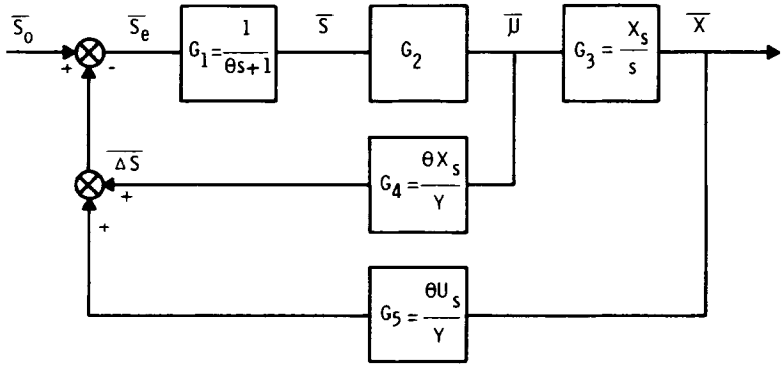

Fig. 2. Block diagram of chemostat.

between $\bar{\mu}$ and $\bar{S}$, that is, in terms of Figure 2, the determination of G_2. Before discussing experimental methods of evaluating G_2, a theoretical consideration of the phenomenon responsible for establishing growth rate of cells in a chemostat should give some insight into the functional nature of G_2. The two phenomena that determine the specific growth rate of cells in a chemostat are mass transport of limiting substrate across the cytoplasmic membrane of the cell and the subsequent biochemical reactions within the cell. If one considers the behavior of an *average cell* in a chemostat population, it is possible to derive equations that suggest mathematical characteristics for G_2. Consider first the active transport of limiting nutrient across the cytoplasmic membrane of the average cell. During a transient period a dynamic relationship exists between S and internal limiting nutrient concentration, S_i. A mass balance on S_i in the *average cell* gives the equation

$$\text{Accumulation} = \text{Input} - \text{Output} - \text{Reacted}$$

$$V_c(dS_i/dt) = J_{in}(S/K_1 + S)V_c - J_{out}(S_i/K_2 + S_i)V_c - \nu(S_i/K_3 + S_i)V_c \qquad (20)$$

where: V_c = cell volume

J_{in} = maximum inward volumetric flux

J_{out} = maximum outward volumetric flux

ν = maximum reaction rate

K_1, K_2, K_3 = saturation constants

Membrane transport studies have shown that active transport net flux is the sum of inward and outward fluxes which follow Michaelis-Menten kinetics.[16] Rearranging equation (17) gives (if $K_2 \simeq K_3$)

$$(1/J_{out} + \nu)(dS_i/dt) + (S_i/K_2 + S_i) = (J_{in}/J_{out} + \nu)(S/K_1 + S) \qquad (21)$$

If it can be assumed that for small perturbations in the chemostat $S \ll K_1$ and $S_i \ll K_2$, equation (21) can be linearized to the deviation equation

$$\tau_T(d\bar{S}_i/dt) + \bar{S}_1 = K_4\bar{S} \qquad (22)$$

where: $\tau_T = (K_2/J_{out} + \nu)$

$$K_4 = (J_{in}/J_{out} + \nu)(K_2/K_1)$$

Equation (22) suggests that the membrane transport step might be approximated by a first order system. Similar theoretical considerations assuming transport could be approximated by simple diffusion have led to first and second order transfer functions for the membrane transport process.[10] Membrane transport studies on *S. cerevisiae* have indicated that the dynamics of membrane transport could be significant in contributing to G_2.[17-24]

Considering the reactions within the cell, the specific growth rate can be expressed by the equation

$$\mu = \nu(S_i/K_3 + S_i) \tag{23}$$

which by previous assumptions concerning K_3 and S_i becomes the deviation equation

$$\bar{\mu} = K_5\bar{S}_i \tag{24}$$

where: $K_5 = (\nu/K_2)$

Taking the Laplace transform of equations (22) and (24) gives respectively

$$(\tau_T s + 1)\bar{S}_i(s) = K_4\bar{S}(s) \tag{25}$$

$$\mu(s) = K_5\bar{S}_i(s) \tag{26}$$

Combining equations (25) and (26) gives the transfer function

$$G_2 = [\bar{\mu}(s)/\bar{S}(s)] = (K/\tau s + 1) \tag{27}$$

where: $K = (K_4/K_5)$

Equation (27) suggests that G_2 can be approximated by a first order transfer function. Similar results were obtained assuming transport by simple diffusion followed by a first order reaction.[10] The reactions within the *average cell* could further contribute to the functional nature of G_2. For example, when the *average cell* in the chemostat experiences an increase in S_i it may not have the extra enzymes available to react S_i at a higher rate. Induction of additional enzymes or activation of enzyme pools may require time. This time delay might be approximated by a transfer function of pure transport delay. Thus, equation (26) could be written as

$$\mu(s) = K_5 e^{-sT}\bar{S}_i(s) \tag{28}$$

From the above considerations a general transfer function for G_2 might be represented by the equation

$$G_2 = [Ke^{-sT}/(\tau s + 1)] \tag{29}$$

It is not intended to imply that equation (29) can be rigidly derived from theory, but rather that theoretical considerations do give a rationale to the use of equation (29) in a dynamic mathematical model of the chemostat.

A General Dynamic Model of the Chemostat

A general dynamic model of the chemostat consists of the equations

$$(dX/dt) = \mu X - DX \tag{1}$$

$$(dS/dt) = DS_o - DS - (\mu X/Y) \tag{2}$$

$$[\bar{\mu}(s)/\bar{S}(s)] = [Ke^{-sT}/(\tau s + 1)] \tag{29}$$

$$\bar{\mu} = \mu - \mu_s \tag{12}$$

$$\bar{S} = S - S_s \tag{11}$$

It should be noted that the model as expressed in the above equations has not been linearized and that equations (1) and (2) are in terms of total variables. The only linearity assumed is found in equation (29) which is written in terms of deviation variables. (An analog simulation of the above equations shown in Figure 7 should illustrate this point.) If equations (1) and (2) are written in deviation variables and linearized to the form of equations (15) and (16) it is then possible to express the model in block diagram form. The block diagram is the same as that of Figure 2 where G_2 is expressed by equation (29). From the block diagram it is possible to calculate the overall transfer functions. Assuming no transport delay ($T = 0$)

$$[\bar{X}(s)/\bar{S}_o(s)] = \{1/s[(\theta_s + 1)(\tau s + 1) + K_1] + K_2\} \tag{30}$$

$$[\bar{S}(s)/\bar{S}_o(s)] = \{s(\tau s + 1)/s[(\theta s + 1)(\tau s + 1) + K_1] + K_2\} \tag{31}$$

Experimental Determination of G_2 Transfer Function

The determination of the transfer function relating $\bar{\mu}$ and $\bar{S}$ in a chemostat can be determined from direct frequency forcing or pulse testing the system. Direct forcing is difficult because sinusoidal

variations in input variables are hard to generate and because the time required for transients to die out is lengthy. Pulse testing the chemostat, on the other hand, is simple and requires much less time than direct forcing while yielding an equivalent amount of frequency response data. A pulse test consists of disturbing an input variable in a predetermined way such that the input variable deviates from steady state for a period of time and then returns to steady state. The response of the output variable or variables is then measured. Hougen[25] has discussed pulse testing in detail. The input-output transient data can be reduced to frequency response data by using a digital program to evaluate Fourier integrals. Clements and Snelle[26] have presented a numerical method which makes use of Filon's quadrature to evaluate the Fourier integrals. At present there are not sufficient experimental data for accurate determination of G_2. A pulse in $\bar{S}$ can be made by a step or square wave change in $\bar{S}_o$. The response of $\bar{\mu}$ can be calculated from the response of X by the equation

$$\bar{\mu} = [(dX/dt)/X] \tag{32}$$

which can be evaluated most accurately by digital computer. Storer and Gaudy[7] have recorded responses of $\bar{\mu}$ to $\bar{S}$ following step changes in $\bar{S}_o$. Reduction of their data to frequency response indicated that G_2 was a first or second order transfer function with a time constant in the range of 40 minutes to one hour and a gain of 0.91 $hr^{-1}/gm/l$. The accuracy of the frequency response data was limited because the frequency content fell off rapidly at frequencies above the corner frequency. Young and Bruley[10] have measured population responses in a chemostat following square wave changes in S_o. In these pulses the normalized frequency content remained high for two decades beyond the break frequency. However, G_2 could not be determined from experimental data because it was found that cell number is not an accurate parameter for cell mass during transient periods. Therefore $\bar{X}_{(t)}$ and $\bar{\mu}_{(t)}$ could not be accurately determined from experimental data. Despite the fact that G_2 was not experimentally determined the results obtained do demonstrate the feasibility of pulse testing the chemostat to obtain frequency response. In Figure 3 a Bode diagram obtained from direct sine forcing; is compared with a Bode diagram obtained by pulse testing. In both cases the chemostat tested was a glucose limited culture of *S. cerevisiae*

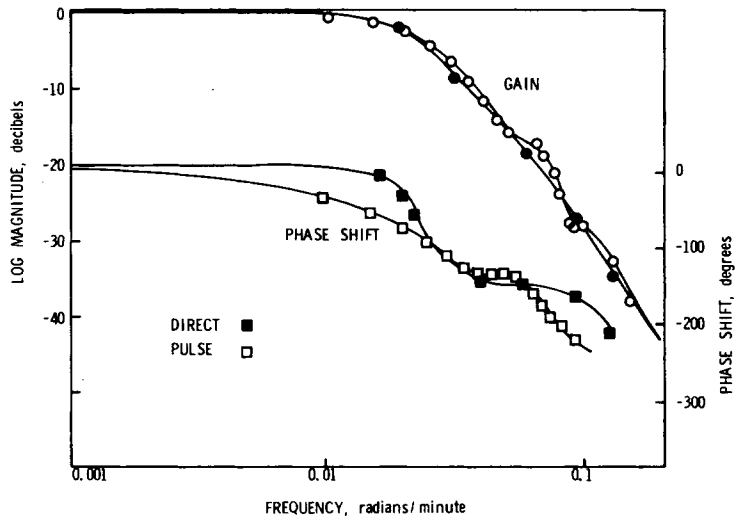

Fig. 3. Comparison of direct sinusoidal forcing[7] and pulse testing[10] frequency response curves for a glucose-limited chemostat of *S. cerevisiae* with a steady state specific growth rate of 0.22 hr^{-1}.

with a steady state specific growth rate of 0.22 hr^{-1}. From Figure 3 it can be seen that agreement is very close, both Bode diagrams indicating a second to third order transfer function with a time constant in the range of 40 minutes. The transfer function plotted from direct forcing is $N(s)/D(s)$ (where N was cell number). The transfer function from pulse testing is $\bar{S}(s)/\bar{S}_o(s)$. It is to be expected that the timing and order of the closed loop response to perturbations in S_o and D should be similar. The direct forcing data also compare favorably with pulse testing frequency responses data shown in Figure 4. Here the transfer function $N(s)/\bar{S}_o(s)$ is shown to be approximately third order with a time constant in the range of 40 minutes to one hour. The linearity of the chemostat over the range tested is also confirmed by Figure 4 which represents the frequency response to pulses in S_o with amplitudes varying from 2 gm/l to 20 gm/l. It can be seen that the response was independent of pulse amplitude as would be expected for a linear system. Finally, it is of interest to compare the responses in Figures 3 and 4 with the transfer functions obtained in equations (30) and (31) by assuming that G_2 was

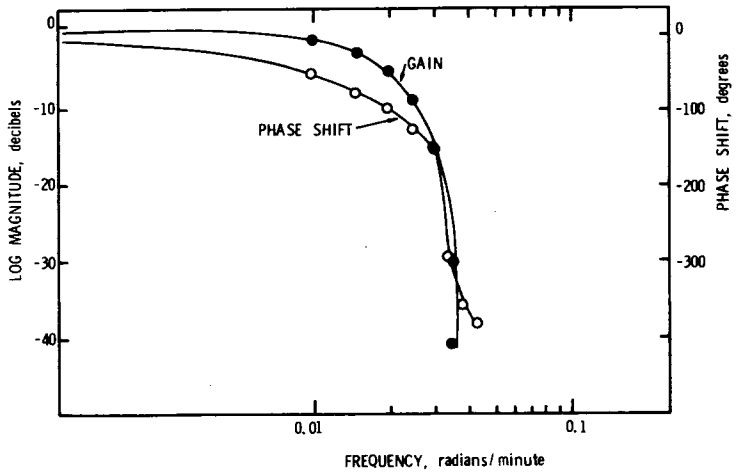

Fig. 4. Pulse testing[10] frequency response determined from 40 minute square wave pulses in S_o from an initial steady state value of 1.0 gm/l to 2.0, 5.0, and 10.0 gm/l.

a first order transfer function. It can be seen from the above equations that $\bar{X}(s)/\bar{S}_o(s)$ and $\bar{S}(s)/S_o(s)$ are third order, a fact that agrees well with the observed Bode plots.

SIMULATION OF DYNAMIC MODELS

In the discussion that follows, the dynamic responses of analog simulations of the newly developed chemostat model are compared with those of the Monod model and with those of experimental chemostats. In attempting to simulate experimental dynamic responses of various chemostats, variations can be made on the above model. The transfer function expressed in equation (29) can be first order, pure transport delay, or a combination of these depending on the values assigned to T and τ. In addition it may be found that in order to get quantitative fits to experimental data the yield coefficient must be made a function of S, dS/dt, or μ.

Dynamic Responses of First Order Model

If T is made to equal zero equation (29) becomes

$$[\bar{\mu}(s)/\bar{S}(s)] = (K/\tau s + 1) \qquad (29')$$

An analog simulation of a hypothetical chemostat operating under the conditions given in Table 1 gave transient responses to step changes in D and S_o as shown in Figures 5 and 6. Here the effect of τ and K on transient response can be seen. An analog simulation of the general dynamic model of the chemostat is given in Figure 7. Monod model responses are given in Figure 8.

TABLE I
Conditions for Growth in a Hypothetical Chemostat

Parameter	Symbol	Value
S. S. dilution rate	D_1	0.20 hr^{-1}
Step change dilution rate	D_2	0.40 hr^{-1}
S. S. specific growth rate	μ_s	0.20 hr^{-1}
S. S. input limiting substrate conc.	So_1	1.0 gm/l
Step input limiting nutrient conc.	So_2	2.0 gm/l
S. S. output limiting nutrient conc.	S_s	0.025 gm/l
S. S. output cell mass conc.	X_s	0.4875 gm/l
Yield coefficient	Y	0.50

Dynamic Response of Transport Delay Model

If $\tau = 0$, equation (29) becomes

$$[\bar{\mu}(s)/\bar{S}(s)] = Ke^{-\tau s} \qquad (29'')$$

Simulated responses using equation (29″) are shown in Figures 9 and 10.

Comparison of General Model and Monod Model with Experimental Data

Responses predicted by the newly developed model and those predicted by the Monod model are compared with responses of experimental chemostats in Figures 11 and 12. In Figure 11 the response to a step change in S_o is shown. The experimental data was presented by Storer and Gaudy.[7] The Monod equation was not accurate in predicting the X response because it did not include a dynamic lag. The general model fitted the X response relatively accurately with parameter values predicted from the experimental data:

$$\tau = 50 \text{ min}$$

$$T = 0$$

$$K = 0.90 \text{ hr}^{-1}/\text{gm/l}$$

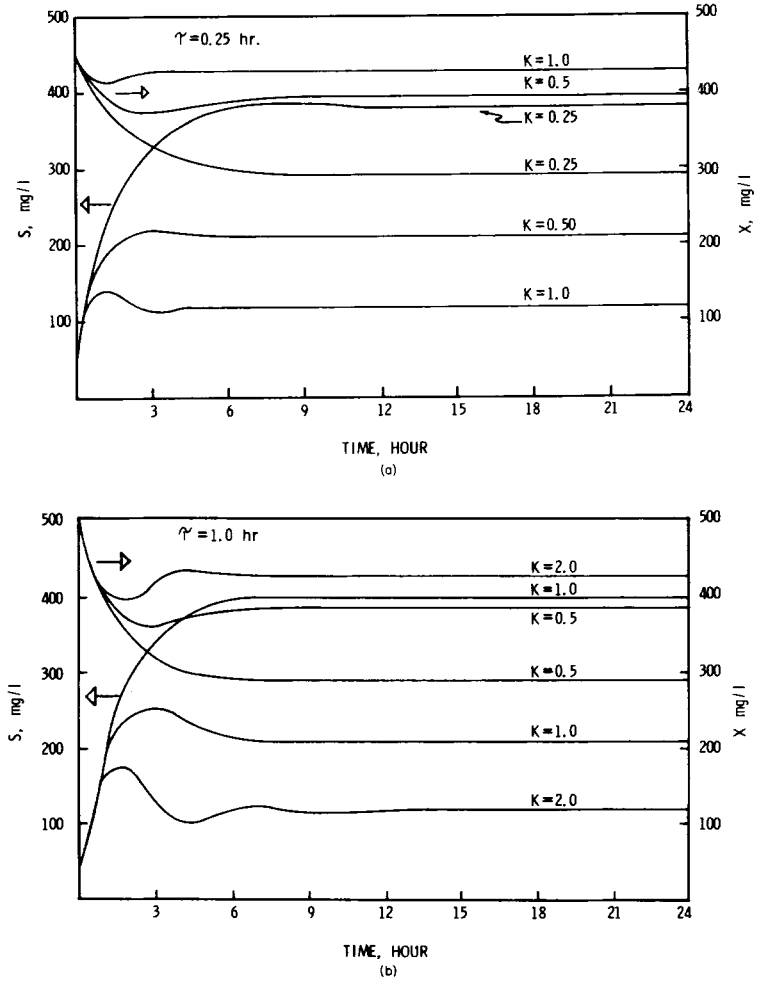

Fig. 5a, 5b. Effect of τ and K on response of a hypothetical chemostat to a step change in D.

Storer and Gaudy[15] found that the yield coefficient varied during the transient period. In the present work, it was found that the variation in yield coefficient during the transient state could be approximated by the equation

$$Y = Y_s - K_y(dS/dt) \tag{33}$$

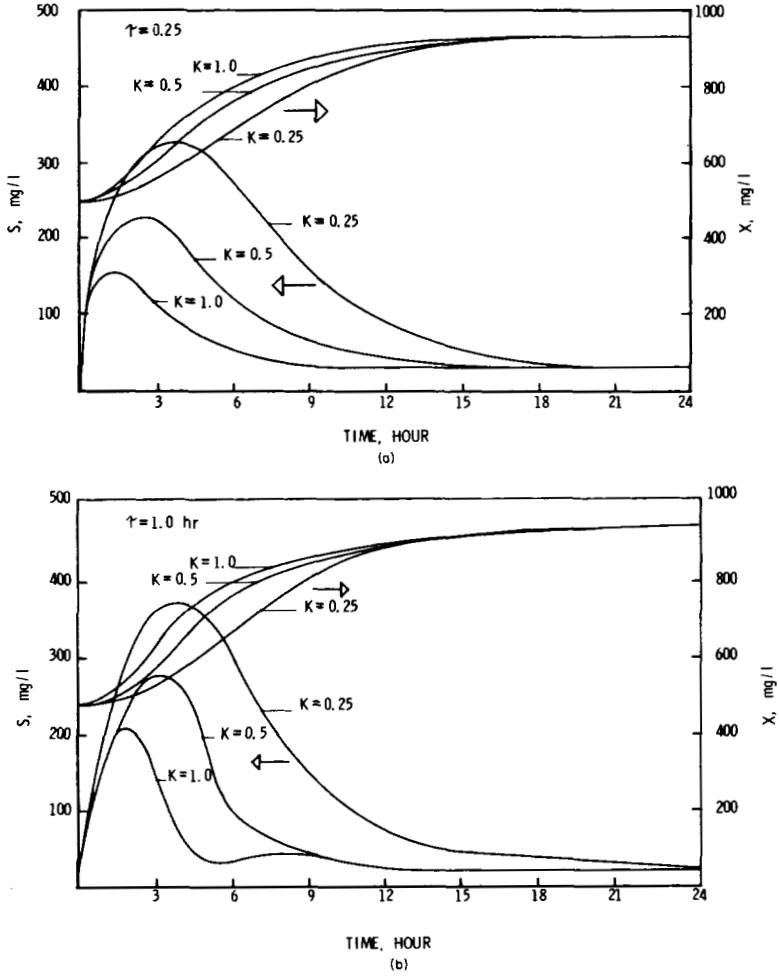

Fig. 6a, 6b. Effect of τ and K on response of a hypothetical chemostat to a step change in S_0.

This improved the accuracy of the predicted S response. In Figure 12 the response to a step change in D is shown. The Monod equation predicts a smooth transition in both X and S from the initial to the new steady state. This is in contrast to the maximum in S and minimum in X observed experimentally by Mateles, Ryu, and Yasuda.[3] The general model was found to approximate the X

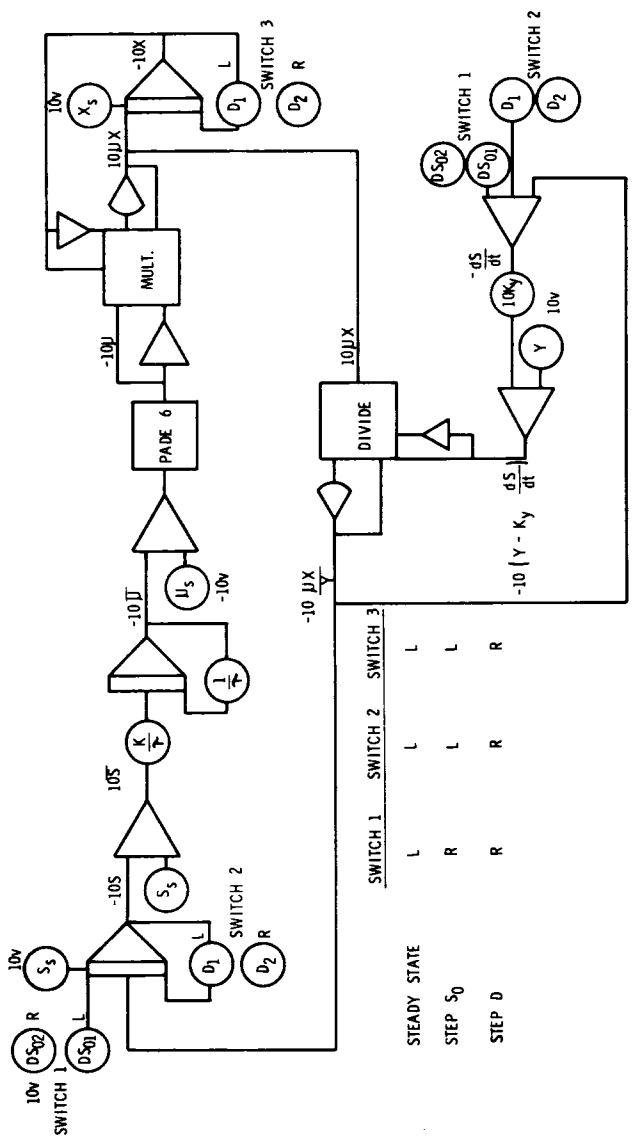

Fig. 7. Analog simulation of dynamic model of the chemostat incorporating first order lag and pure transport delay circuits. Circuit in lower right corner accounts for variation in Y during transient as given in equation (33).

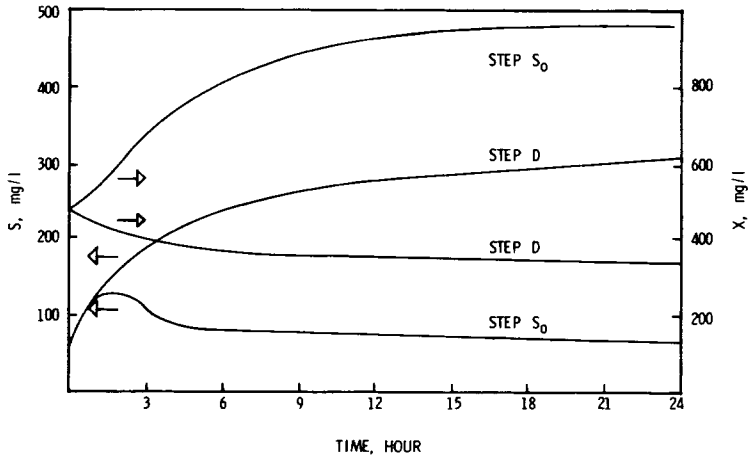

Fig. 8. Chemostat response to step changes in S_o and D as predicted by basic Monod model.

response and to fit the μ response, but the S response predicted a higher value at steady state than was observed experimentally. The parameter values used were as follows:

$$\tau = 20 \text{ min}$$

$$T = 0$$

$$K = 3.0 \text{ hr}^{-1}/\text{gm}/1$$

DISCUSSION

In review of the ideas presented here a few points merit further discussion. It has been argued on the basis of theoretical considerations and experimental data that the Monod equation is not valid during transient states in a chemostat resulting from perturbations in steady state. Furthermore, it has been suggested that in such transient situations the Monod equation should be replaced by a time dependent equation; i.e., equation (29). It is not unlikely that the linearity assumed between $\bar{\mu}$ and $\bar{S}$ in equation (29) will be questioned. Also, the use of frequency response techniques to determine the parameters in equation (29) will likely be criticized for the same reason. However, the fallacy in such criticisim is that it assumes the chemostat to be dynamically nonlinear on the basis of nonlinear steady state data. Such thinking views the transient

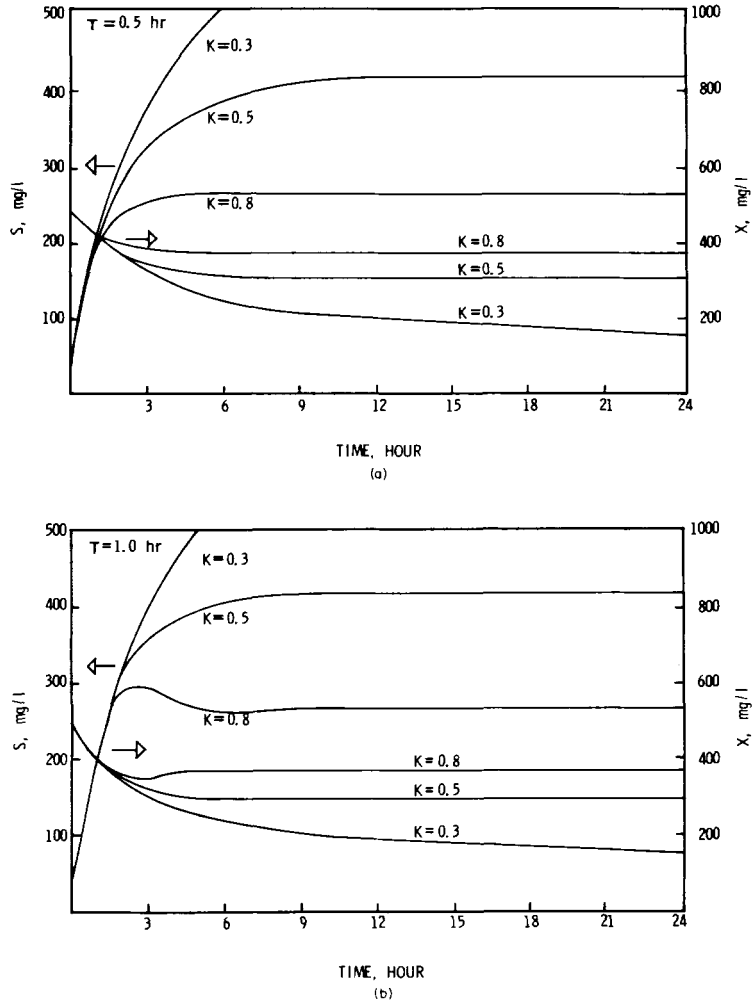

Fig. 9a, 9b. Effect of T and K on response of a hypothetical chemostat to a step change in D.

response of μ as following along a nonlinear Monod curve when in fact the transient growth rate response does not necessarily follow the Monod curve at all. The only way to answer the question of linearity in the dynamic case is by perturbing the limiting substrate concentration over a range of amplitudes and observing the growth

rate responses. Then and only then can any valid statements be made concerning linearity in the dynamic case. Without such information it is assumed that within a range of perturbations the growth rate responds linearly. This assumption can be justified if

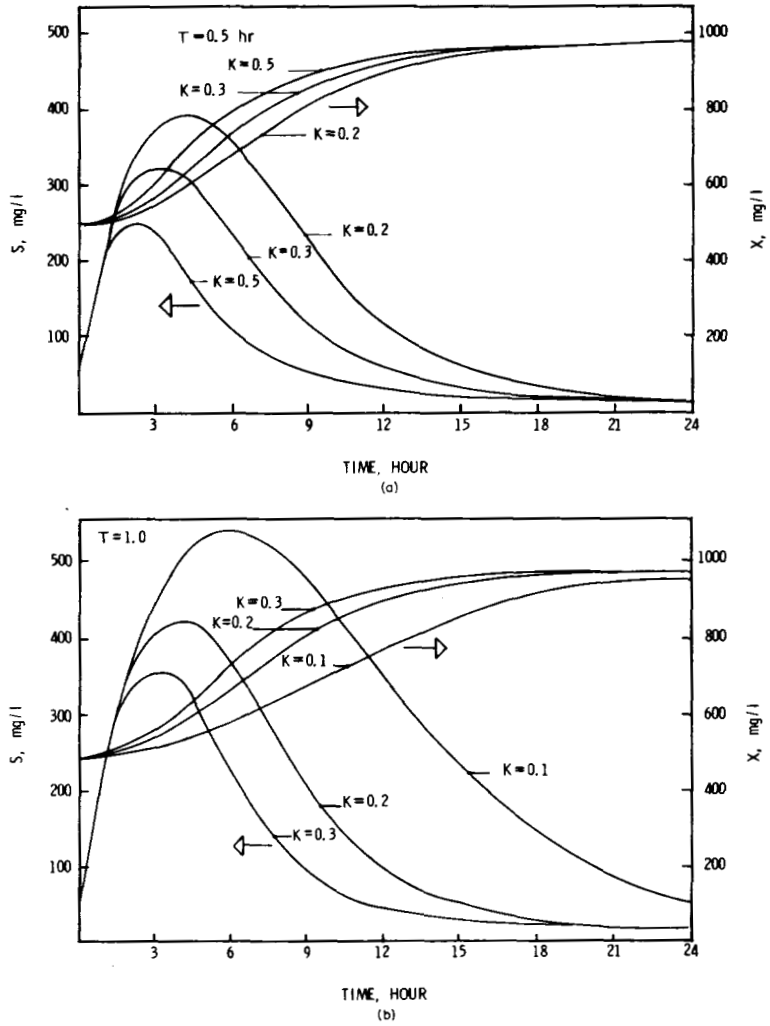

Fig. 10a, 10b. Effect of T and K on response of a hypothetical chemostat to a step change in S_o.

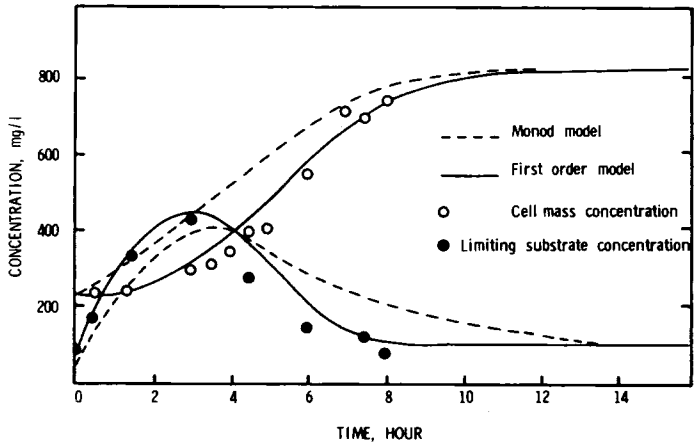

Fig. 11. Comparision of responses predicted by Monod model and by first order model (equation (29″)) with experimental data of Storer and Gaudy.[15]

simulated responses compare well quantitatively with experimental transient data.

CONCLUSIONS

In summary of the present work the following conclusions are made:

1. The Monod model is not accurate in predicting the transient behavior of experimental chemostats. This is not surprising since the Monod equation is not a time dependent dynamic equation.
2. A systems engineering approach can be useful in developing dynamic mathematical models of the chemostat. The dynamic relationship between μ and S can be determined from experimentally pulse testing the chemostat to get frequency response data.
3. A general model of the chemostat consists of the equations

$$(dX/dt) = X - DX \tag{1}$$

$$(dS/dt) = DS_o - DS - (\mu X/Y) \tag{2}$$

$$\bar{\mu} = \mu - \mu_s \tag{12}$$

$$\bar{S} = S - S_s \tag{11}$$

$$[\bar{\mu}(s)/\bar{S}(s)] = [Ke^{-Ts}/(\tau s + 1)] \tag{26}$$

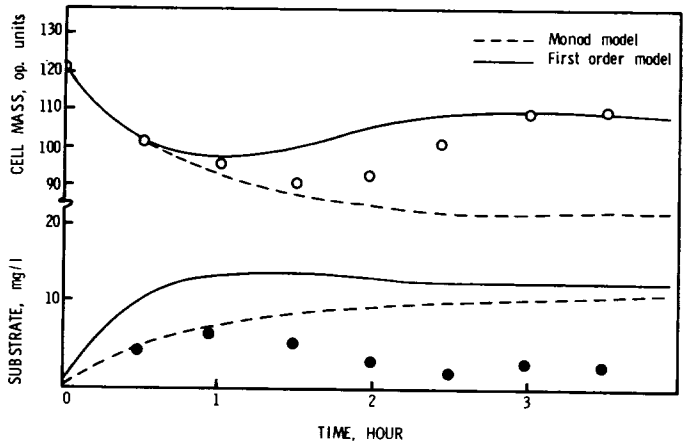

Fig. 12. Comparison of responses predicted by Monod model and by first order model (equation (29′)) with experimental data of Mateles *et al.*[11]

The parameters T, τ, and K can be varied to predict the transient response of chemostats to perturbations in D and S_o. An additional equation to account for variations in Y during transients may be formulated with Y as a function of S and t or μ and t.

4. At present there are not sufficient experimental data available to clearly define or to generalize on the dynamic behavior of the chemostat. Consequently, it is not yet possible to generalize on the relationship developed here between μ and S. However, the results of simulations presented here would indicate that a model incorporating a first order transfer function relating $\bar{\mu}$ and $\bar{S}$ is accurate in predicting the dynamic behavior of experimental chemostats.

References

1. J. F. Andrews, *Biotechnol. Bioeng.*, **10,** 707 (1968).
2. S. Koga and A. E. Humphrey, *Biotechnol. Bioeng.*, **9,** 37 (1967).
3. R. I. Mateles, D. Y. Ryu, and T. Yasuda, *Nature*, **208,** 263 (1965).
4. S. Aiba, S. Nagai, Y. Nishizawa, and M. Onodera, *J. Gen. Appl., Microbiol.* **13,** 73 (1967).
5. S. Aiba, S. Nagai, Y. Nishizawa, and M. Onodera, *J. Gen. Appl. Microbiol.*, **13,** 85 (1967).
6. S. Nagai, Y. Nishizawa, I. Endo, and S. Aiba, *J. Gen. Appl. Microbiol.*, **14,** 121 (1968).

7. F. F. Storer and A. F. Gaudy, *Environ. Sci. Technol.*, **3,** 143 (1969).
8. J. W. Gilley and H. R. Bungay, *Biotechnol. Bioeng.*, **9,** 617 (1967).
9. J. W. Gilley and H. R. Bungay, *Biotechnol. Bioeng.*, **10,** 99 (1968).
10. T. B. Young and D. F. Bruley, "A Theoretical and Experimental Dynamic Analysis of a Continuous Culture of Yeast," MS Thesis, Dept. of Ch E, Clemson Univ., Clemson, S. C. (1968).
11. T. Yasuda and R. I. Mateles, Paper presented at 148th meeting ACS, Chicago, Ill., Abstracts of papers, 18Q (1964).
12. C. J. Perret, *J. Gen. Microbiol.*, **22,** 589 (1960).
13. D. Herbert, R. Elsworth, and R. C. Telling, *J. Gen. Microbiol.*, **14,** 601 (1956).
14. S. Aiba, S. Nagai, I. Endo, and Y. Nishizawa, *AICHE Journal*, **15,** 624 (1969).
15. E. O. Powell, Microbial Physiology and Continuous Culture, Third Int. Symposium, Porton Down, Salisbury, and Wiltshire, England, Her Majesty's Stationery Office (1967).
16. W. D. Stein, "The Movement of Molecules across Cell Membranes," 137, Academic Press, New York and London (1967).
17. V. P. Cirillo, *J. Bacteriol.*, **84,** 485 (1962).
18. J. Van Stevenick and A. Rothstein, *J. Gen. Physiol.*, **49,** 235 (1965).
19. J. Van Stevenick, *Biochim. Biophys. Acta*, **126,** 154 (1966).
20. J. Van Stevenick, *Biochim. Biophys. Acta*, **150,** 47 (1968).
21. J. Van Stevenick, *Biochim. Biophys. Acta*, **150,** 424 (1968).
22. J. Van Stevenick, *Biochim. Biophys. Acta*, **163,** 386 (1968).
23. J. Van Stevenick and H. L. Booij, *J. Gen. Physiol.*, **48,** 43 (1964).
24. P. O. Wilkins and V. P. Cirillo, *J. Bacteriol.*, **90,** 1905 (1965).
25. J. O. Hougen, "Experiences and Experiments in Process Dynamics," CEP Monograph Series, No. 4, **60,** (1964).
26. W. C. Clements and K. B. Snelle, I & EC Process Design and Development, 2, 94 (1963).

Received July 7, 1970
Revised July 10, 1970